PHOTOELASTIC ANALYSIS OF A HYDRAULIC GEAR PUMP HOUSING

by

Joseph P. Rudinec

Submitted in Partial Fulfillment of the Requirements

for the Degree of

Master of Science in Engineering

in the

Mechanical Engineering

Program

[illegible] May 24, 1973

Adviser Date

Frank J. Tarantine May 24, 1973

Adviser Date

[illegible] May 30, 1973

Dean of the Graduate School Date

YOUNGSTOWN STATE UNIVERSITY

June, 1973

ABSTRACT

PHOTOELASTIC ANALYSIS OF A HYDRAULIC GEAR PUMP HOUSING

Joseph P. Rudinec

Master of Science in Engineering

Youngstown State University, 1973

The purpose of this investigation was to experimentally determine the stresses in a hydraulic gear pump housing (using the photoelastic stress freezing technique), and to recommend criteria for future designs.

The gear housing is considered as a plane stress problem with difficulties in an analytical solution that arise from the complex shape, method of restraint, and the dependence of the internal pressure distribution upon the rotational speed of the pump.

A full scale housing model was machined from a suitable photoelastic material, and assembled into a pump. This pump model was then operated at a scaled pressure load while subjected to the stress freezing cycle.

A slice from the model was analyzed using conventional photoelastic techniques. The maximum stress was determined, and recommendations were made to reduce this stress level.

TABLE OF CONTENTS

CHAPTER I

INTRODUCTION

The trend in the mobile hydraulics industry toward constantly increasing operating pressures, while demanding smaller components of increased capacity, makes it essential for designers to accurately predict the behavior of present as well as future designs of hydraulic components.

External gear pumps of the type shown in Figure 1, are widely used in the hydraulic power systems to provide a continuous transfer of the fluid. Operation of the pump is shown schematically by Figure 2. Two gears (contained inside the gear housing) are made to rotate. This transfers the fluid trapped between the gear teeth from the inlet to the outlet. Reverse flow of the fluid is restricted by the gear mesh, sealing between the gear tips and the housing, and sealing between the gear faces and the thrust plates.

The pump selected for analysis was a Commercial Shearing Inc. model P75A-1½. This is the medium gear width in a very popular series. The unit is rated at 2400 rpm and 2500 psi, which is typical in the American mobile hydraulics industry.

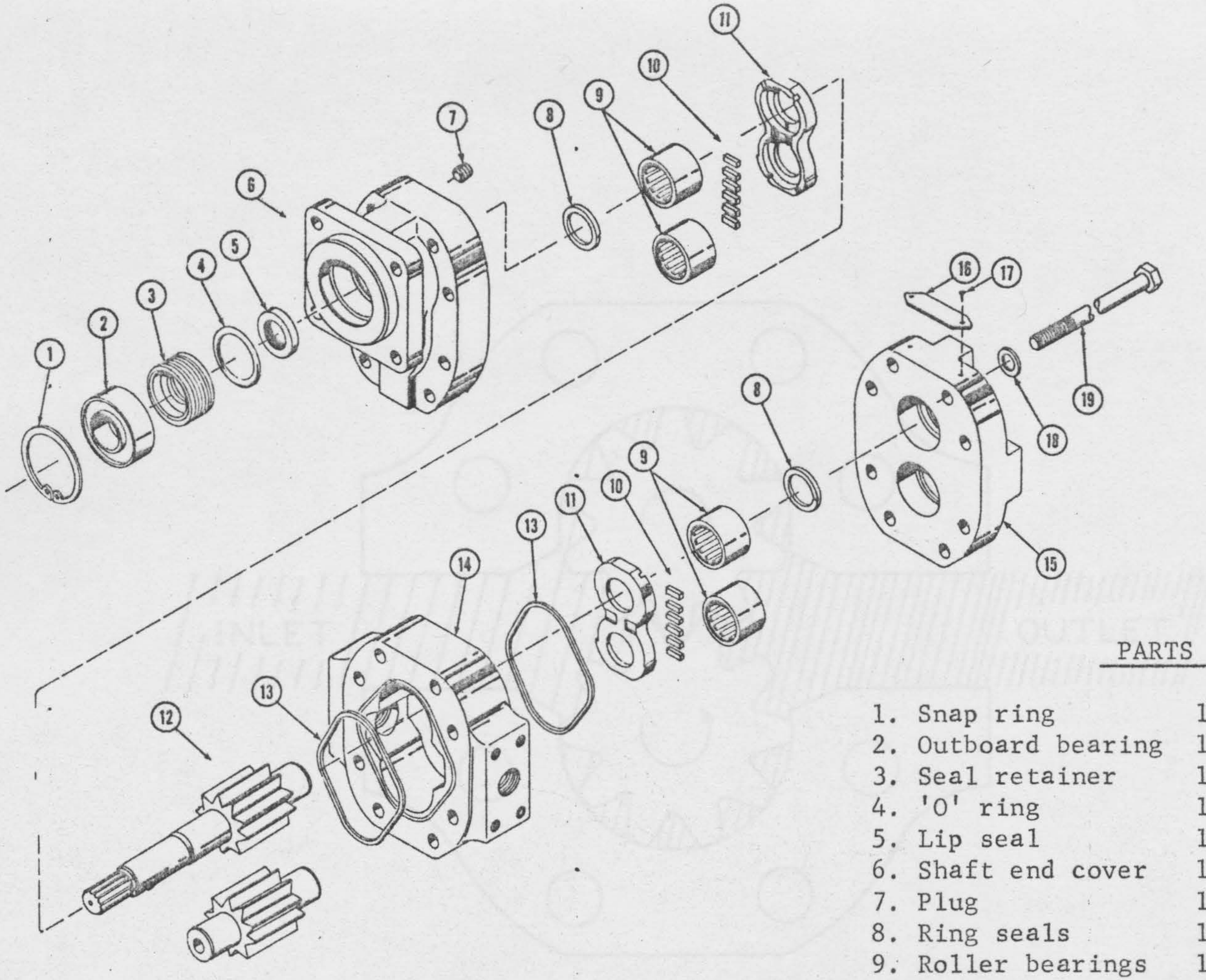

PARTS LIST

1. Snap ring
2. Outboard bearing
3. Seal retainer
4. 'O' ring
5. Lip seal
6. Shaft end cover
7. Plug
8. Ring seals
9. Roller bearings
10. Pocket seals
11. Thrust plates
12. Gear set
13. Section rings
14. Gear housing
15. Port end cover
16. Name plate
17. Drive screws
18. Washers
19. Bolts

COMMERCIAL SHEARING, INC.

P 75

Fig. 1.--Exploded view of a Commercial Shearing Inc. P75

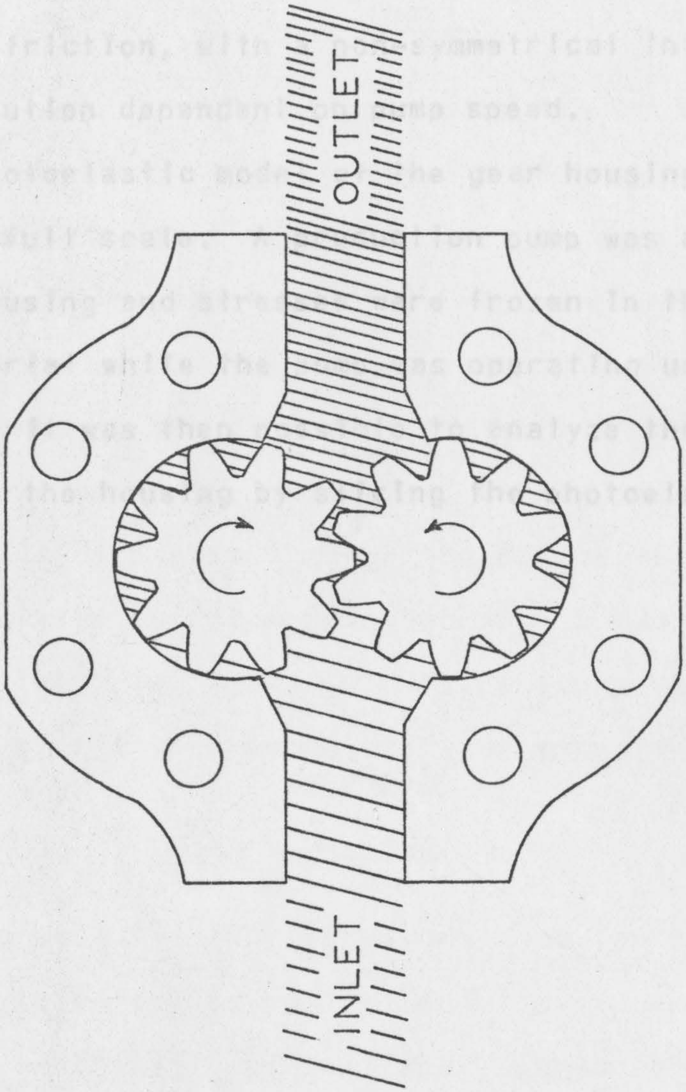

Fig. 2.--Schematic of gear pump operation

It is seen in Figure 2 that external gear pumps are inherently unbalanced by the pressure differential across the gears. This causes several problems, one of which is the stress in the gear housing. The difficulty in mathematical analysis occurs since the housing is a complex shape, restrained by friction, with a non-symmetrical internal pressure distribution dependent on pump speed.

A photoelastic model of the gear housing was constructed to full scale. A production pump was assembled with this housing and stresses were frozen in the photoelastic material while the pump was operating under scaled conditions. It was then possible to analyze the stress on any plane in the housing by slicing the photoelastic model.

CHAPTER II

ESTABLISHMENT OF TEST PARAMETERS

The Circuit

The test circuit for operating the model is shown schematically in Figure 3. The fluid (Ambrex 97K from Mobil Oil Co.) is drawn into the model by partial vacuum as indicated by the pressure gauge P_1. The flow out of the model is restricted by the needle valves V_1 and V_2. This causes the pump to see an outlet pressure which is indicated by P_2. A portion of the pump flow, as regulated by the setting of V_2, is channeled through the heat exchanger, cooled, and combined with the flow going through V_1 which is then returned to the tank. The fluid temperature for the system is recorded by the thermocouple T_1 suspended in the tank.

The Model

When establishing a pressure load for the model, emphasis was placed on having the load low enough to prevent rupture or significant deformations. Conversely, the load must be high enough to establish fringes of an order that can be analyzed. One point cannot be overemphasized--if the load

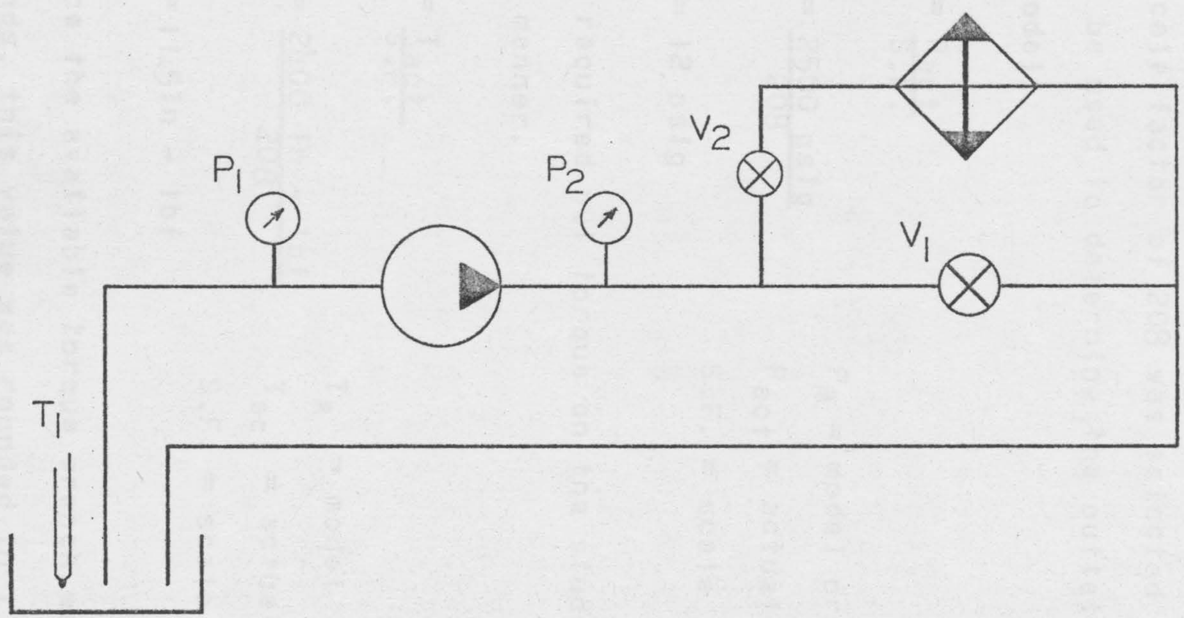

Fig. 3.--Schematic of test circuit

is low and no fringes or significant deformations can be detected prior to slicing, it is possible to rerun the model at an increased load; whereas, rupture or large deformations invalidate the test data and would require the construction of a new model in order to rerun the test.

A scale factor of 208 was selected as being adequate. It can then be used to determine the outlet pressure of the operating model.

$$P_m = \frac{P_{act}}{S.F.}$$

$$P_m = \frac{2500 \text{ psig}}{208}$$

$$P_m = 12 \text{ psig}$$

P_M = model pressure, psig

P_{act} = actual pressure, psig

S.F. = scale factor, 208

The required nut torque on the studs is determined in the same manner.

$$T_M = \frac{T_{act}}{S.F.}$$

$$T_M = \frac{2400 \text{ in - lbf}}{208}$$

$$T_M = 11.5 \text{ in - lbf}$$

T_M = model torque, in-lbf

T_{act} = actual torque, in lbf

S.F. = scale factor, 208

Since the available torque wrench was calibrated in foot pounds, this value was rounded to 1 foot pound (12 in. - lbf).

Since the material used for the housing model (Photoelastic, PLM-4B) is susceptible to creep at stress freezing temperatures, it is advisable to spring load the nuts to insure the force will be maintained. This was accomplished as shown in Figure 4.

The following spring was selected since it fits nicely over the stud and between the washers, has an acceptable spring constant, and was readily available.

CS inc.	Part No.------------	A1327-320
	Rate----------------	202 lbf/in.
	OD------------------	1.00 in.
	Wire dia.----------	.156 in.
	Free length--------	2.541 in.
	Solid length-------	1.404 in.

It was experimentally determined that 12 in.-lbf of nut torque would compress the spring to a length of 1.9125 inches. Then all eight springs were set to this length assuring uniform forces. To facilitate spring installation and to provide a means of anchoring the model to the oven, the studs were selected to extend between one and two inches beyond the compressed springs.

Inlet and outlet ports (both 1 inch N.P.T.) as well as taps for the pressure gauges ($\frac{1}{4}$ inch N.P.T.) were located in the port end cover.

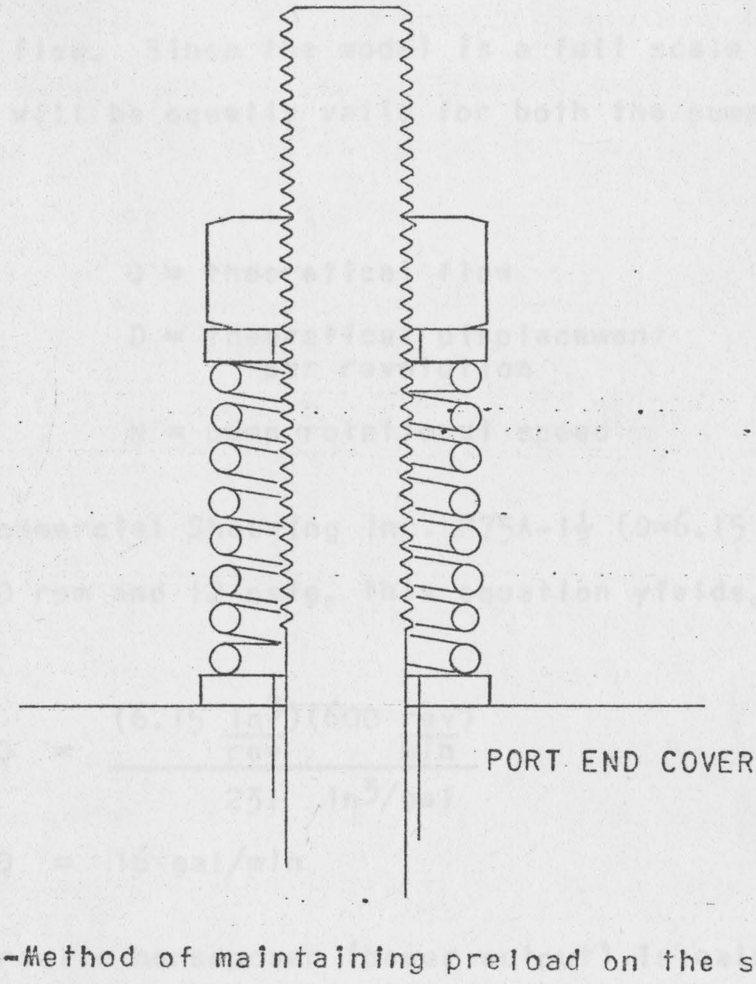

Fig. 4.--Method of maintaining preload on the studs

The Motor

The horsepower requirements to drive the loaded model can be determined using SAE formulae. At low pressure, the internal slip loss is zero and the pump delivery is equal to the theoretical flow. Since the model is a full scale pump, these equations will be equally valid for both the pump and the model.

$Q = D*N$

Q = theoretical flow

D = theoretical displacement per revolution

N = pump rotational speed

For a Commercial Shearing Inc. P75A-1½ (D=6.15 $in.^3$/rev) operating at 600 rpm and 12 psig, this equation yields,

$$Q = \frac{(6.15\ \frac{in^3}{rev})(600\ \frac{rev}{min})}{231\ \ in^3/gal}$$

$$Q = 16\ gal/min$$

The hydraulic horsepower (power output) is calculated as,[1]

$$\text{Hyd HP} = \frac{(gpm)(psig)}{1714}$$

$$^{1}HP = \frac{gal}{min} * \frac{231\ in^3}{gal} * \frac{lbf}{in^2} * \frac{1 ft}{12\ in} * \frac{1\ HP}{33,000\ lbf/min}$$

$$HP = \frac{gpm * psi}{1714}$$

A production unit of this type generally operates with an overall efficiency of 85% or more at rated speed and pressure (2400 rpm and 2500 psi). However, at low pressures, this efficiency can drop to 50% or less. This occurs here since power is required to overcome internal friction and at low pressures, there is very little hydraulic power output. Assuming a 50% overall efficiency, the approximate input horsepower is then calculated:

$$\text{Input HP} = \frac{\text{Hydraulic HP}}{\text{Over-all Eff.}}$$

$$\text{Input HP} = \frac{(.112\ \text{HP})}{.5}$$

$$\text{Input HP} = .224\ \text{HP}$$

Noting that power losses are incurred in the drive train (shown schematically in Figure 5), and the fact that the model must be operated continuously for six days under load, a one-horsepower motor was determined to be suitable (this yields a safety factor of 4).

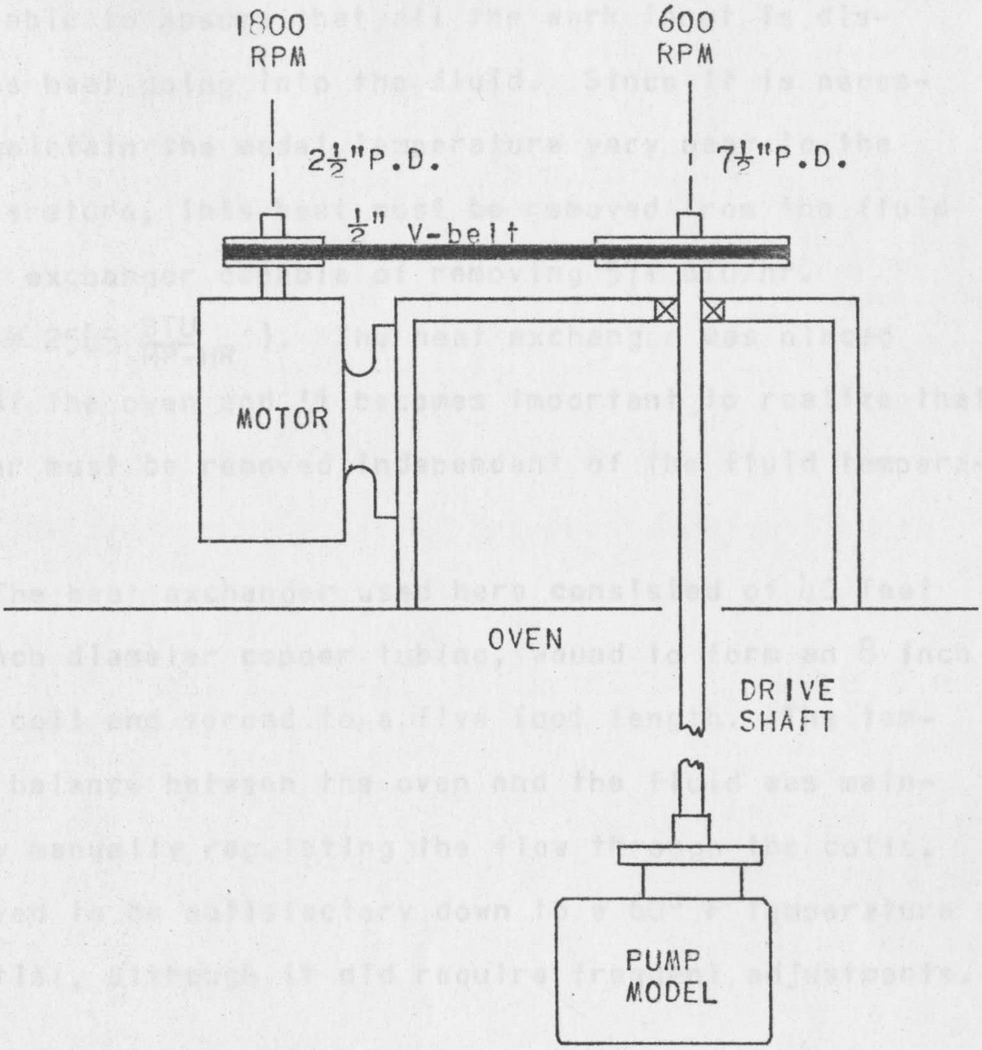

Fig. 5.--Schematic of the drive train

The Heat Exchanger

The model pump does no useful work; therefore, it is reasonable to assume that all the work input is dissipated as heat going into the fluid. Since it is necessary to maintain the model temperature very near to the oven temperature, this heat must be removed from the fluid by a heat exchanger capable of removing 571 BTU/hr. ($.224$ HP $*$ $2545 \frac{BTU}{HP\text{-}HR}$). The heat exchanger was placed outside of the oven and it becomes important to realize that 571 BTU/hr must be removed independent of the fluid temperature.

The heat exchanger used here consisted of 40 feet of .25 inch diameter copper tubing, wound to form an 8 inch diameter coil and spread to a five foot length. The temperature balance between the oven and the fluid was maintained by manually regulating the flow through the coils. This proved to be satisfactory down to a 60° F temperature differential, although it did require frequent adjustments.

The Oven

The oven, Photolastic Model P-2307-M, was used for this test after the following modifications were made:

1. The rear window was removed to permit running a line to and from the heat exchanger. (This is accomplished by removing all the retaining screws and carefully lifting out the window, noting that the glass panes are loose). A styrofoam block was cut to replace the window and presented no problem with heat loss.
2. The vents on the top of the oven were removed to permit mounting the speed reducer and provide a means to insert the drive shaft.

The components were then mounted as shown in Figure 6.

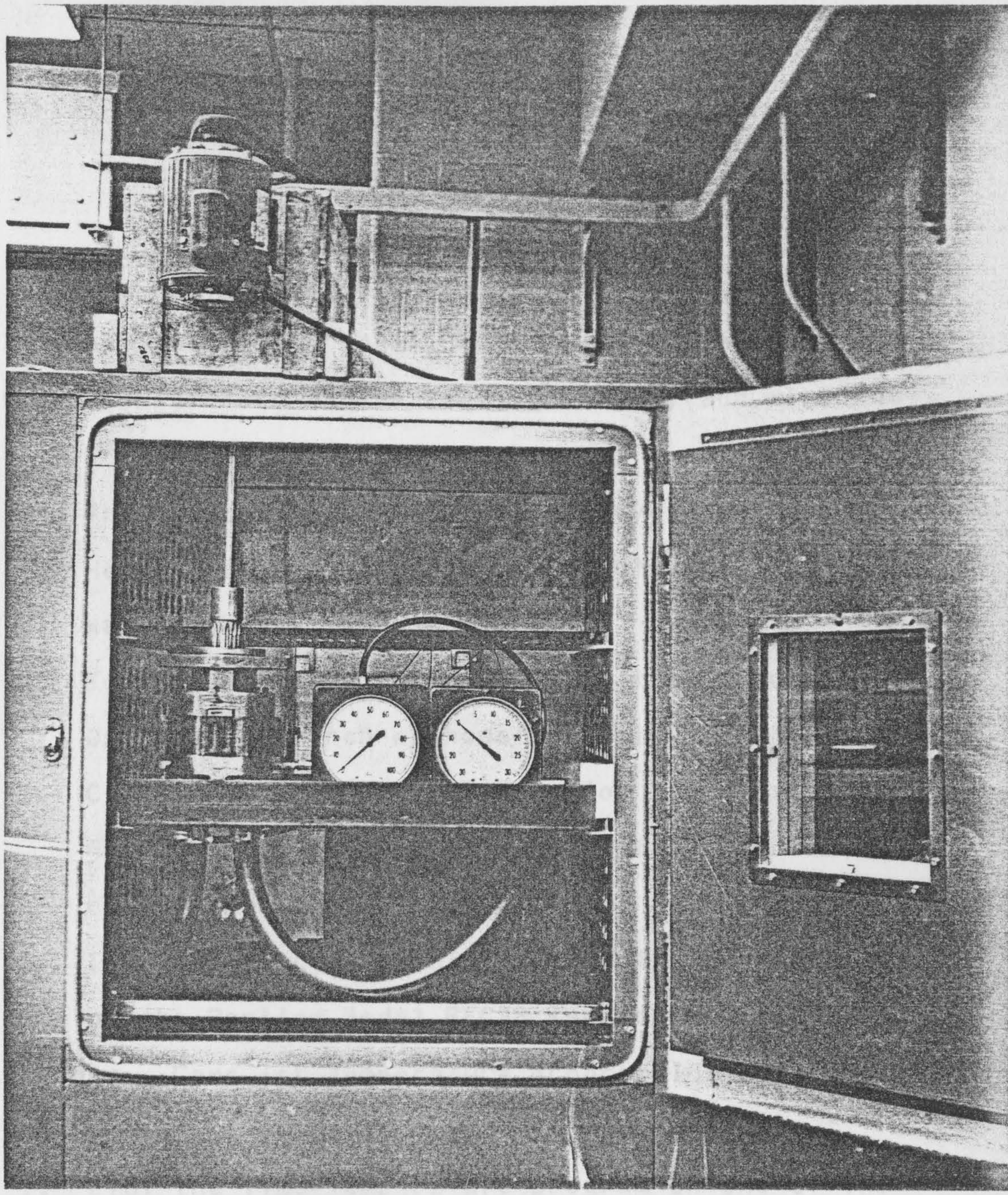

Fig. 6.--Photograph of test assembly

CHAPTER III

TEST PROCEDURES

The entire stress freezing operation can be summarized as loading the model, heating to slightly above the critical temperature of the epoxy (PLM-4B), and slow cooling while maintaining the load.

The following time-temperature cycle was used:

1. Heating at a rate of 10° F/hr until 230° F was reached.
2. Soaking the model at 230° F for three hours. One hour per inch of housing width.
3. Cooling at a rate of 1° F/hr for the first 50° F. Then cooling at a rate of 3° F/hr to room temperature.

Temperature control of the oven is regulated through the use of the Partlow Model RFCSS Recording Temperature Programmer. Cams for temperature programming are constructed in the following manner:

1. Plot the time-temperature program on one of the paper charts supplied. Connect these points with a smooth curve. Illustrated as curve A in Figure 7.

2. On curve A, draw a series of connected 3/8" diameter circles (B).
3. Draw the smooth curve C tangent to the circles.
4. Using rubber cement, glue the chart to a sheet of 1/8" plastic.
5. Drill a $\frac{1}{2}$" diameter center hole, and cut the plastic to conform to curve C.

It proved helpful to leave the chart paper glued to the plastic cam. This provided a reference to the time-temperature cycle making it easier to determine the time for cam changes.

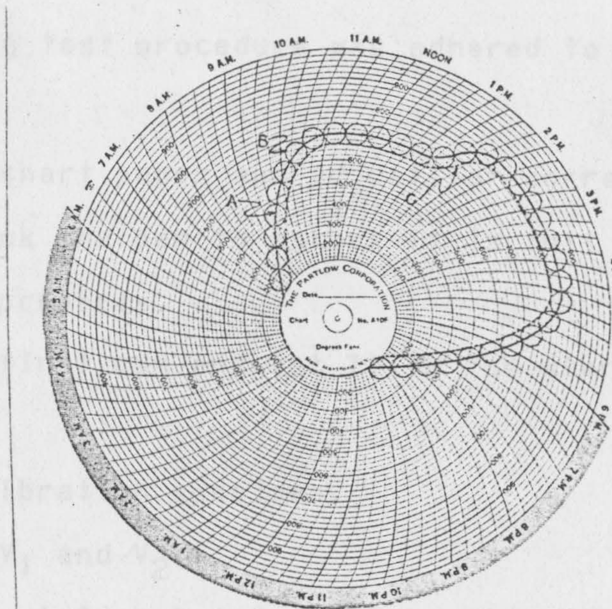

Fig. 7.--Layout of the time-temperature program

Prior to the actual stress freezing, the circuit was tested with a production pump. This was done in an attempt to determine the effect viscosity changes have on outlet pressure, and the amount valve V_1 must be adjusted for compensating purposes.

The following test procedure was adhered to and appeared satisfactory:

1. Install new chart paper and adjust for correct time of day. Check the pen to assure it is full of ink and writing properly.
2. Install the first cam and set it to the start of the cycle.
3. Load the calibration specimen.
4. Open valves V_1 and V_2.
5. Check the electric motor for alignment and start it.
6. Close V_2 one-quarter of a turn.
7. Adjust V_1 to obtain a reading of 12 psig.
8. Set the percentage timer to 100%.
9. Set the heat input to maximum.
10. Turn the oven on and depress the reset button.
11. Turn on the Partlow Programmer.
12. Monitor outlet pressure and oil temperature, resetting whenever necessary.

CHAPTER IV

EVALUATION OF TEST DATA

The Polariscope

The technique of photoelastic stress analysis can be used to provide the following information:

1. The directions of the principal stresses. These are seen as isoclinic (black) lines when the specimen is viewed through a plane polariscope. The isoclinic lines can be seen to move as the analyzer is rotated.
2. The difference between the principal stresses. These are the isochromatic lines and are clearly visible through a circular polariscope. The magnitude of the stress difference is calculated as

$$| \sigma_1 - \sigma_2 | = NF$$

where N = Fringe order

F = Fringe value of the epoxy resin

A collimated light polariscope, shown in Figure 8, was used in the analysis. It was adjusted for use as a dark field circular polariscope with a monochromatic light source. The loading frame (supplied with the polariscope) served to position and support the model.

The photographs used in the final analysis were obtained by placing the camera as shown in Figure 8. The proper exposure was determined by aiming a light meter (set to measure reflected light) at the model.

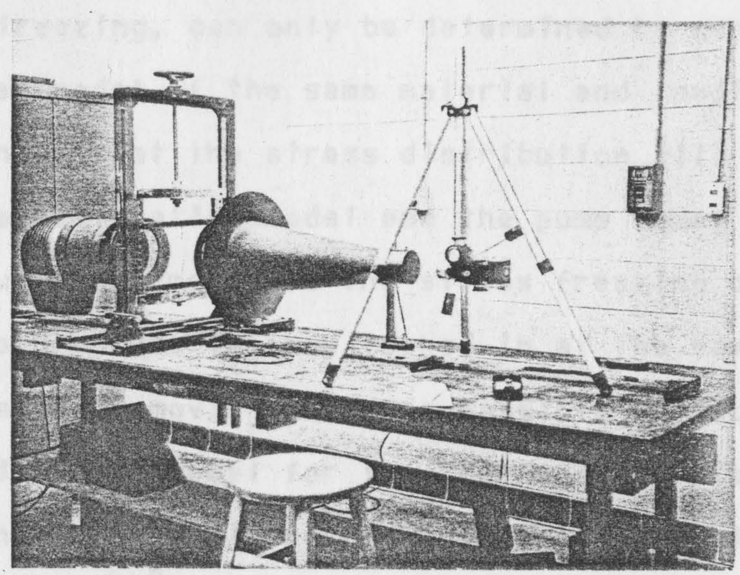

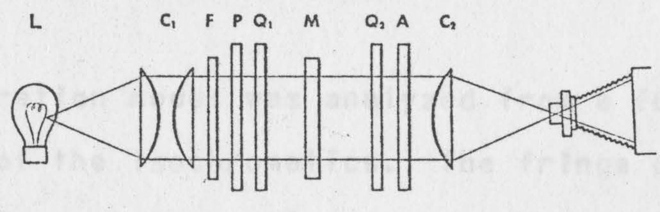

Fig. 8 - Elements of a Polariscope.

L - light source;
C_1 and C_2 - condensers;
F - filter;
P - polarizer;
Q_1 and Q_2 - quarter-wave plates;
M - model;
A - analyzer.

The Calibration

The exact properties of the epoxy resin, at the time of stress freezing, can only be determined by constructing another model of the same material and loading it in such a manner that the stress distribution will be known. Both the calibration model and the pump model are then simultaneously subjected to the stress freezing cycle. The stress in both models is then locked in at the same time and temperature, removing these as possible variables.

The calibration model for the test was the simple tensile specimen shown in Figure 9. The tensile specimen was selected since it's loading was stable even with the slight vibration of the oven produced by driving the pump model.

The calibration model was analyzed from a full-scale photograph of the isochromatics. The fringe order was determined at various cross sections by counting fringes (Figure 10) on overlay number 1 and the stress was then calculated. Plotting the stress as a function order (Figure 11) it can be seen they are linearly related.

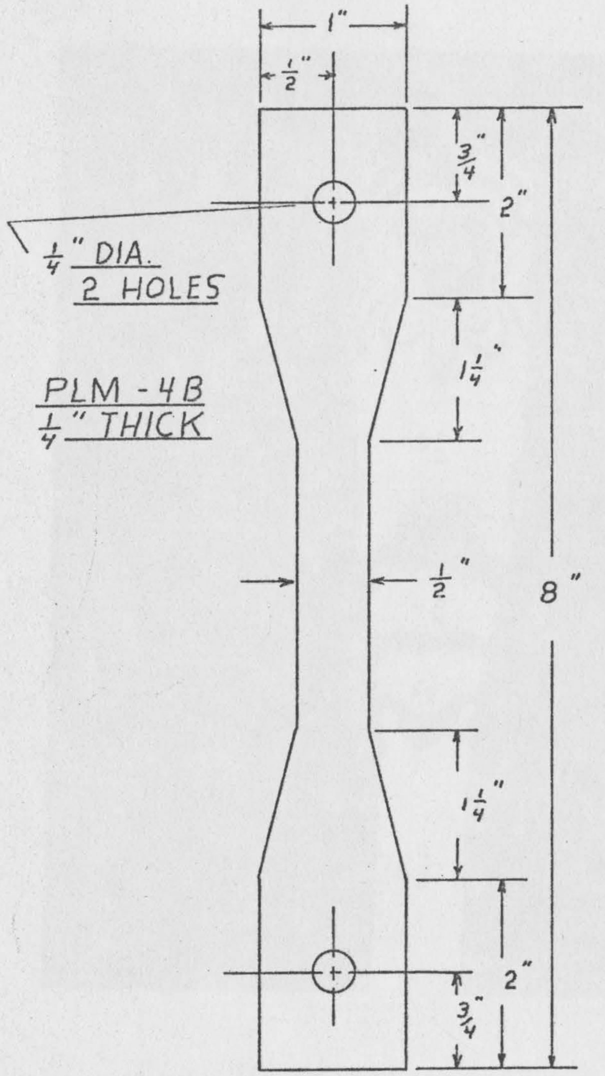

Fig. 9.--The calibration model

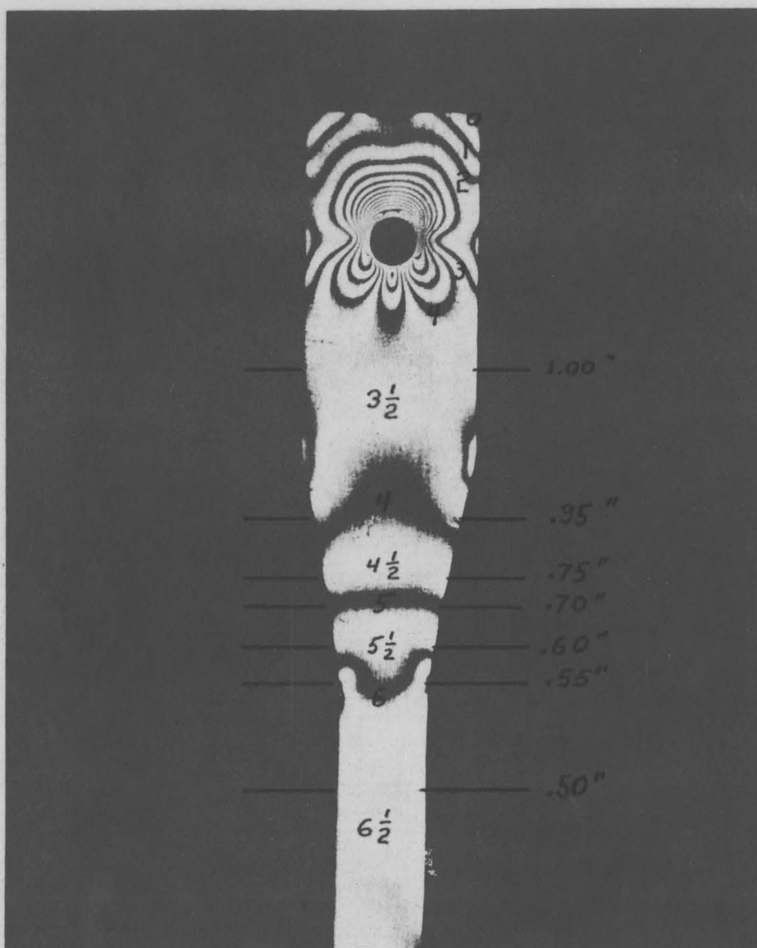

Fig. 10.--Isochromatic fringe pattern in the calibration model

OVERLAY NO. I

IDENTIFICATION OF THE FRINGES

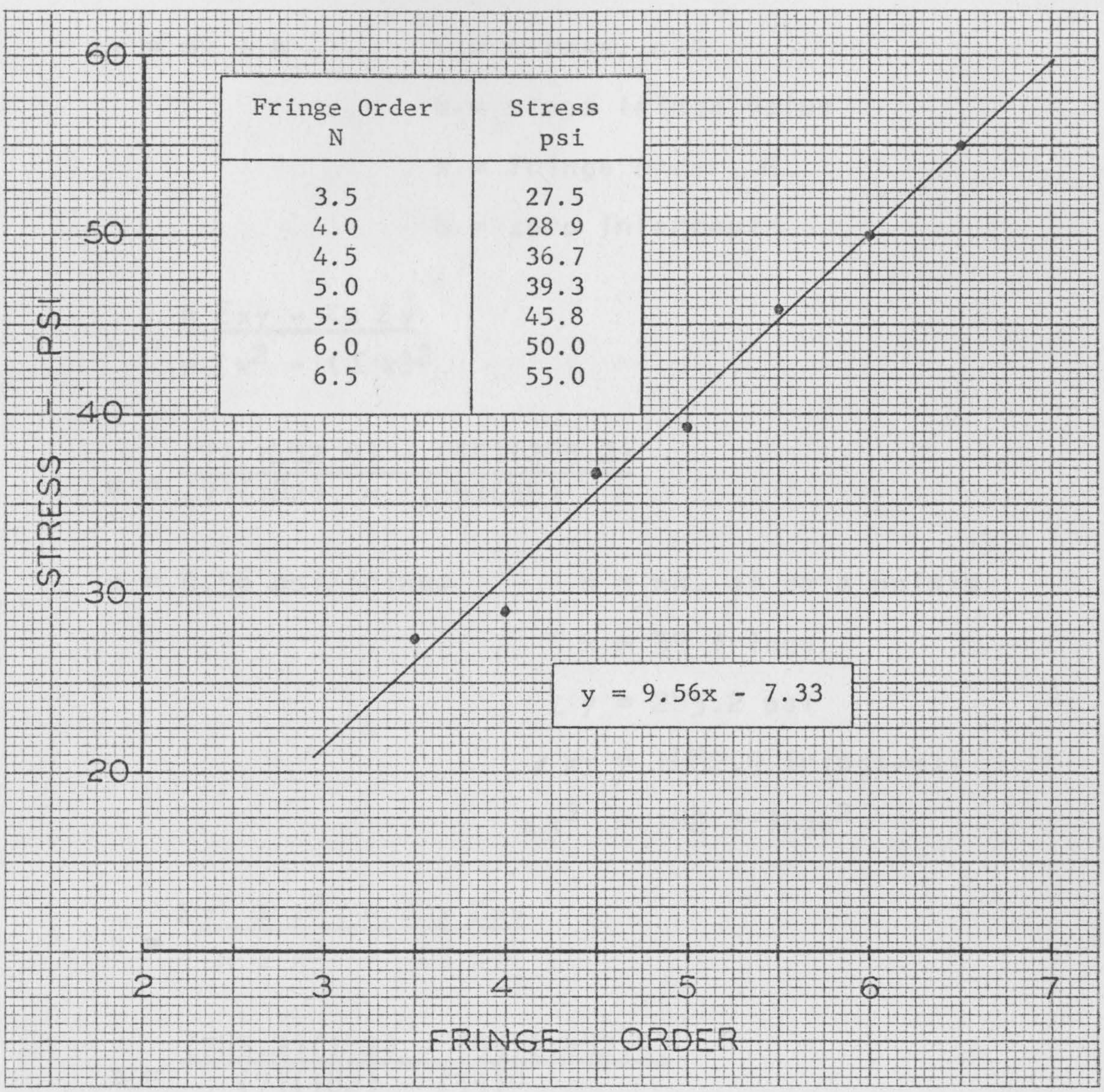

Fringe Order N	Stress psi
3.5	27.5
4.0	28.9
4.5	36.7
5.0	39.3
5.5	45.8
6.0	50.0
6.5	55.0

Fig. 11.--Calibration of the photoelastic material (PLM-4B)

The equation of the best-fit straight line between these data points was determined by the Least Squares Method. That is for the equation:

$y = mx + b$ $\quad$ y = stress, psi

m = slope fringe value

x = fringe order, N

b = zero intercept

$$m = \frac{n \Sigma xy - \Sigma x \Sigma y}{n \Sigma x^2 - (\Sigma x)^2}$$

$$m = \frac{(7)(1482.9) - (35)(283.2)}{(7)(182) - (35)(35)}$$

$m = 9.56$ psi/fringe $\quad$ n = no. of data points

$\Sigma x = 35$ fringe

$\Sigma y = 283.2$ psi

$\Sigma xy = 1482.9$ fringe-psi

$\Sigma x^2 = 182$ fringe^2

$$b = \frac{\Sigma y \ \Sigma x^2 - \Sigma x \Sigma xy}{n \Sigma x^2 - (\Sigma x)^2}$$

$$b = \frac{(283.2)(182) - (35)(1482.9)}{(7)(182) - (35)^2}$$

$b = -7.33$ psi

The equation of the best-fit straight line becomes

$$y = 9.56x - 7.33$$

or

$$\sigma_{psi} = 9.56\ (N) - 7.33$$

The Model

The pressure distribution in an actual pump operating at 600 rpm with an outlet pressure of 1950 psig is illustrated in Figure 12.[2] This indicates that the pressure increases from inlet pressure to 95% of outlet pressure within an angle of 40 degrees ($20^\circ \leq \theta \leq 60^\circ$) and then gradually increases to full outlet pressure in the next 100 degrees ($60^\circ \leq \theta \leq 160^\circ$). Since the housing model is a full-scale gear housing made from an epoxy, it is reasonable to assume the same pressure distribution (although scaled to a lower pressure) will be present when running the model.

---

[2]Commercial Shearing Inc., Report No. 7512-110C Pressure Distribution Around a P75 Gear, Nov. 19, 1970, Carl M. Singer.

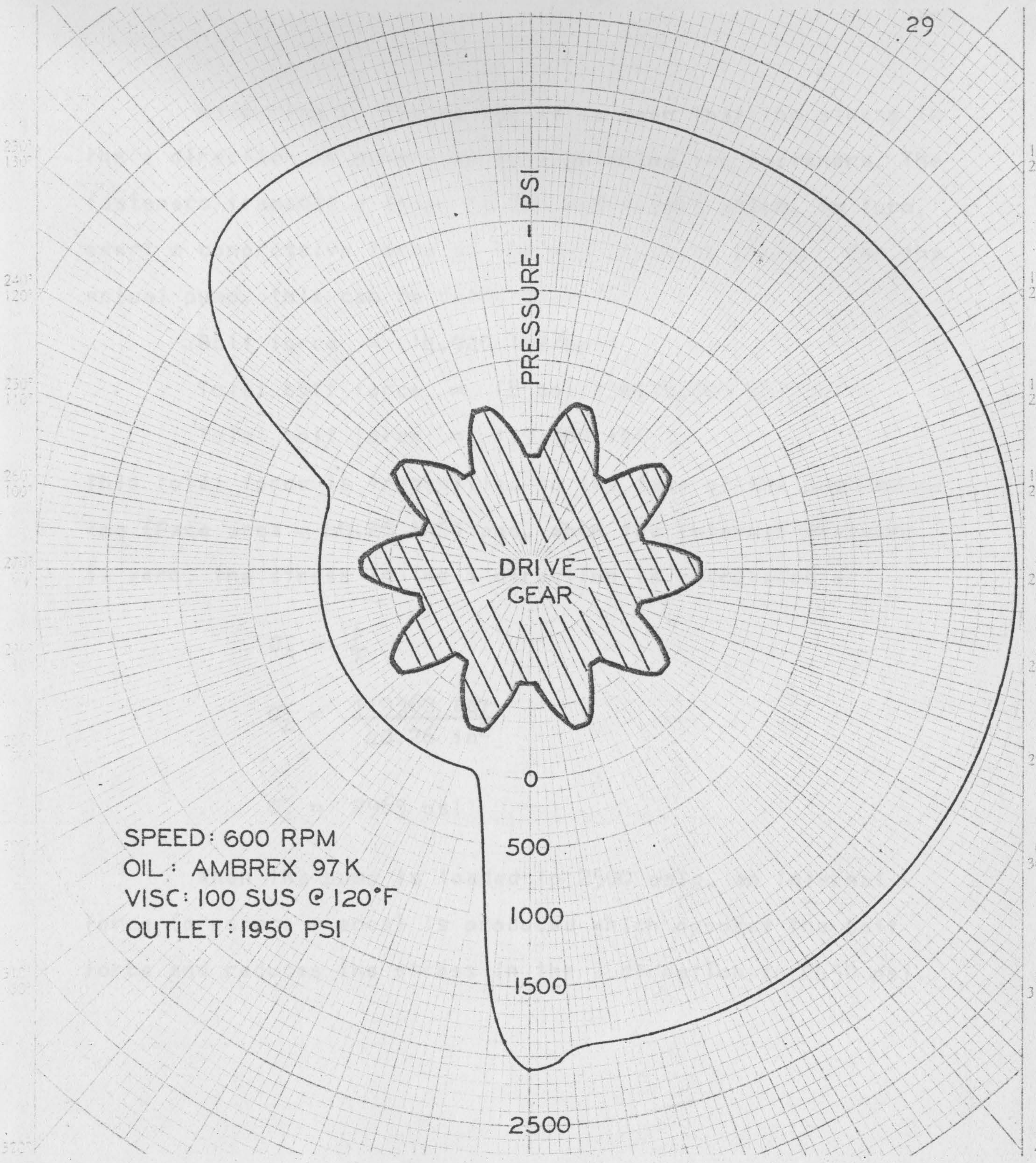

Fig. 12.--Gear pressure distribution

Referring to Figure 13, it is seen that the stress in the z direction is generated by tightening the fasteners. The fasteners transmit a force to the end covers which, in turn, exert a compressive force on the gear housing faces. For the actual pump, this can be calculated as[3]

Bolt force = 14,920 lbf/bolt

Total bolt force = (8 bolts)*(14,920 lbf/bolt)

Total bolt force = 119,360 lbf

This total force is transmitted to the face of the gear housing (Face area = 40.26 in^2) and, when the internal pressure is zero, the stress in the z direction is calculated as

$$\sigma_z = \frac{F}{A}$$

$$\sigma_z = \frac{119360 \text{ lbf}}{40.26 \text{ in}^2}$$

$$\sigma_z = 2965 \text{ psi}$$

When the pump is loaded to 2500 psig, an internal force (pressure * area) is produced which opposes the bolt force and reduces the stress in the z direction to 2450 psi.

[3]Commercial Shearing Inc., Analytical Stress Analysis of a "P" Series Pump, Feb. 12, 1971, Joe Rudinec.

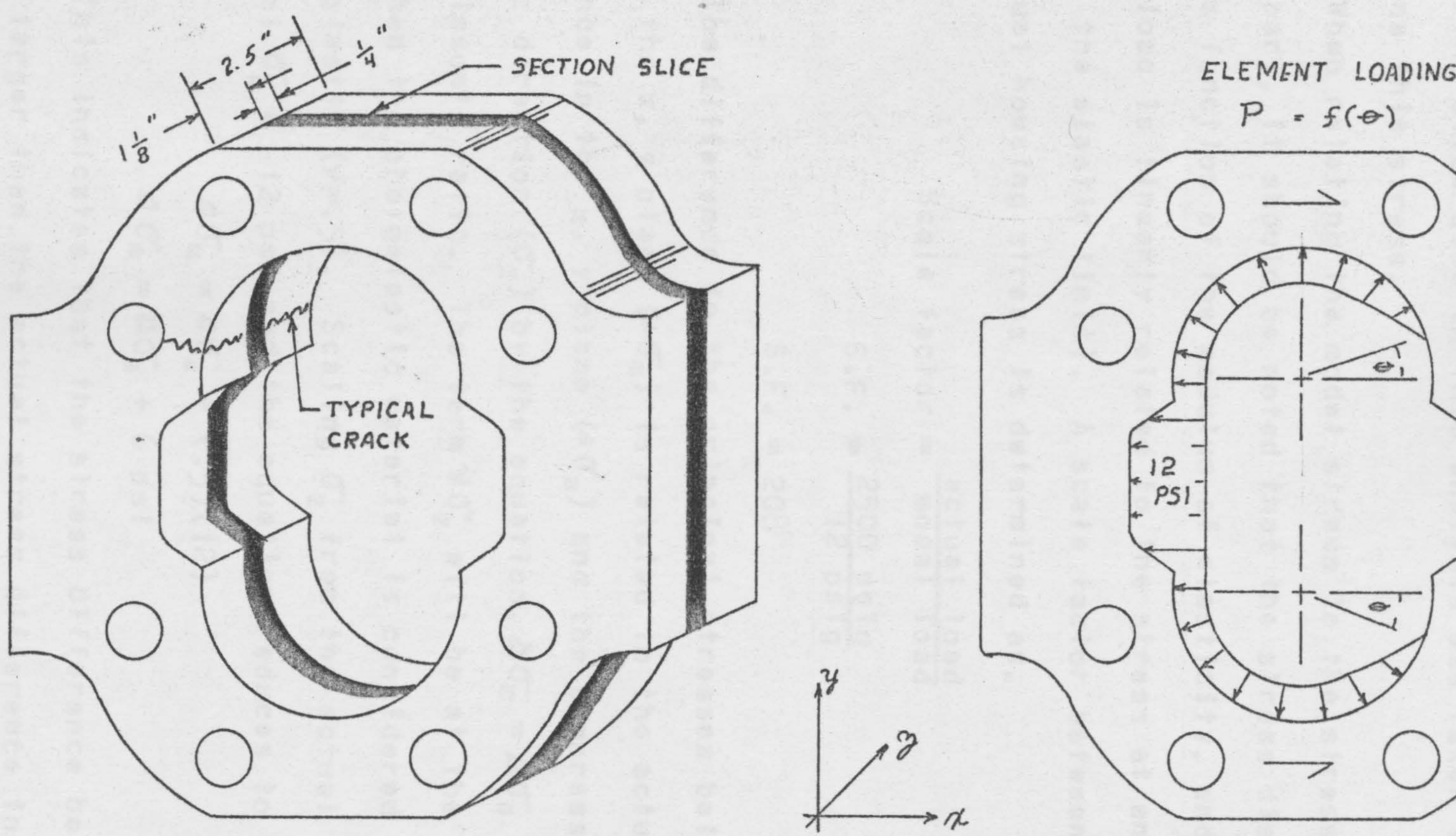

Fig. 13.--Model slice used in the photoelastic analysis

Failure of an actual non-ported gear housing is characterized by a crack as shown in Figure 13. This can be used as an indication that the maximum stress occurs in the x, y plane. The slice used in this analysis was taken in order to determine this stress.

When relating the model stress to the stress in the actual part, it should be noted that the stress distribution is not a function of the modulus of elasticity, and the stress at one load is linearly related to the stress at another (within the elastic limit). A scale factor between the model and actual housing stress is determined as,

$$\text{Scale factor} = \frac{\text{actual load}}{\text{model load}}$$

$$\text{S.F.} = \frac{2500 \text{ psig}}{12 \text{ psig}}$$

$$\text{S.F.} = 208$$

The difference in the principal stresses being measured in the x, y plane ($\Delta\sigma_m$) is related to the actual stress difference in the x, y plane ($\Delta\sigma_a$) and the compressive stress in the z direction (σ_z) by the equation, $\Delta\sigma_m = \Delta\sigma_a - \nu\sigma_z$ where ν is Poisson's ratio. The term $\nu\sigma_z$ will be at the maximum value when the photoelastic material is considered to be perfectly plastic (ν=.5). Scaling σ_z from the actual part to the model σ_z = -12 psi and the equation reduces to

$$\Delta\sigma_m = \Delta\sigma_a + (.5)(12)$$

$$\Delta\sigma_m = \Delta\sigma_a + 6 \text{ psi}$$

This indicates that the stress difference being measured is larger than the actual stress difference in the x, y plane (by 6 psi) and the assumption of plane stress ($\Delta\sigma_m = \Delta\sigma_a$) will indicate stress differences that are larger than actual. For a $\Delta\sigma_a \gg 5.9$ psi, the error introduced by assuming plane stress will be small (for a sixth order fringe this amounts to 12%).

The stress in the gear housing is calculated as,

Actual stress = scale factor * model stress

For example, a sixth order fringe in the model indicates a differential stress of

$$y = 9.56x - 7.33$$

$$y = (9.56)(6) - 7.33$$

$$y = 50 \text{ psi (model)}$$

The scale factor is used to relate model stress (at a 12 psig load) to actual stress (at a 2500 psig load). The actual stress differential can then be calculated,

Actual stress = scale factor * model stress

$$\Delta\sigma_{act} = 208 * 50 \text{ psi}$$

$$\Delta\sigma_{act} = 10{,}400 \text{ psi}$$

Since the fringe order in the model indicates the difference between the principal stresses ($\sigma_1 - \sigma_2$), the individual components of stress can only be determined if one of them is already known (or determined by oblique incidence). If the free surfaces are considered, the principal stresses on the surface are tangent and normal to the

TABLE I

TABULATION OF DIFFERENTIAL STRESS IN THE MODEL AND THE ACTUAL HOUSING

MODEL		PROTOTYPE (SF = 208)
Fringe Order N	$(\sigma_1 - \sigma_2)$ PSI	$(\sigma_1 - \sigma_2)$ PSI
1	2.2	458
1.5	7.0	1456
2	11.8	2454
2.5	16.6	3453
3	21.4	4451
3.5	26.1	5429
4	30.9	6427
4.5	35.7	7426
5	40.5	8424
5.5	45.25	9412
6	50.0	10400
6.5	54.8	11398
7	59.6	12397
7.5	64.4	13395

point of interest. It is noted that the stress normal to the surface is equal to the pressure on the surface, and for free surfaces, σ_2 will be equal to zero.

The stress difference $(\sigma_1 - \sigma_2)$ is tabulated in Table I for both the model and the actual part (scale factor or 208) as a function of the fringe order in the model.

The isochromatic fringe pattern is shown in Figure 14. The fringe orders were identified by counting the fringes, and recorded on overlay number 2. The highest order fringes are located on the inside surfaces of the bolt holes numbered 1, 5 and 2, 6. Hole number 5 has a fringe order of 9 (which was the highest) but on close inspection, it is suspected that this occurred from the housing contacting the bolt. This would cause an abnormally high fringe order at the point of contact and will cause this data point to be neglected.

The loading on the model is symmetric with respect to the horizontal centerline and it is possible to concentrate the analysis on the top half of the housing and neglect the section containing bolt 5. Studying the fringe pattern around hole number 1, it appears that a slight bolt contact may have occurred here. The effect of the contact appears to be small and will, therefore, be neglected.

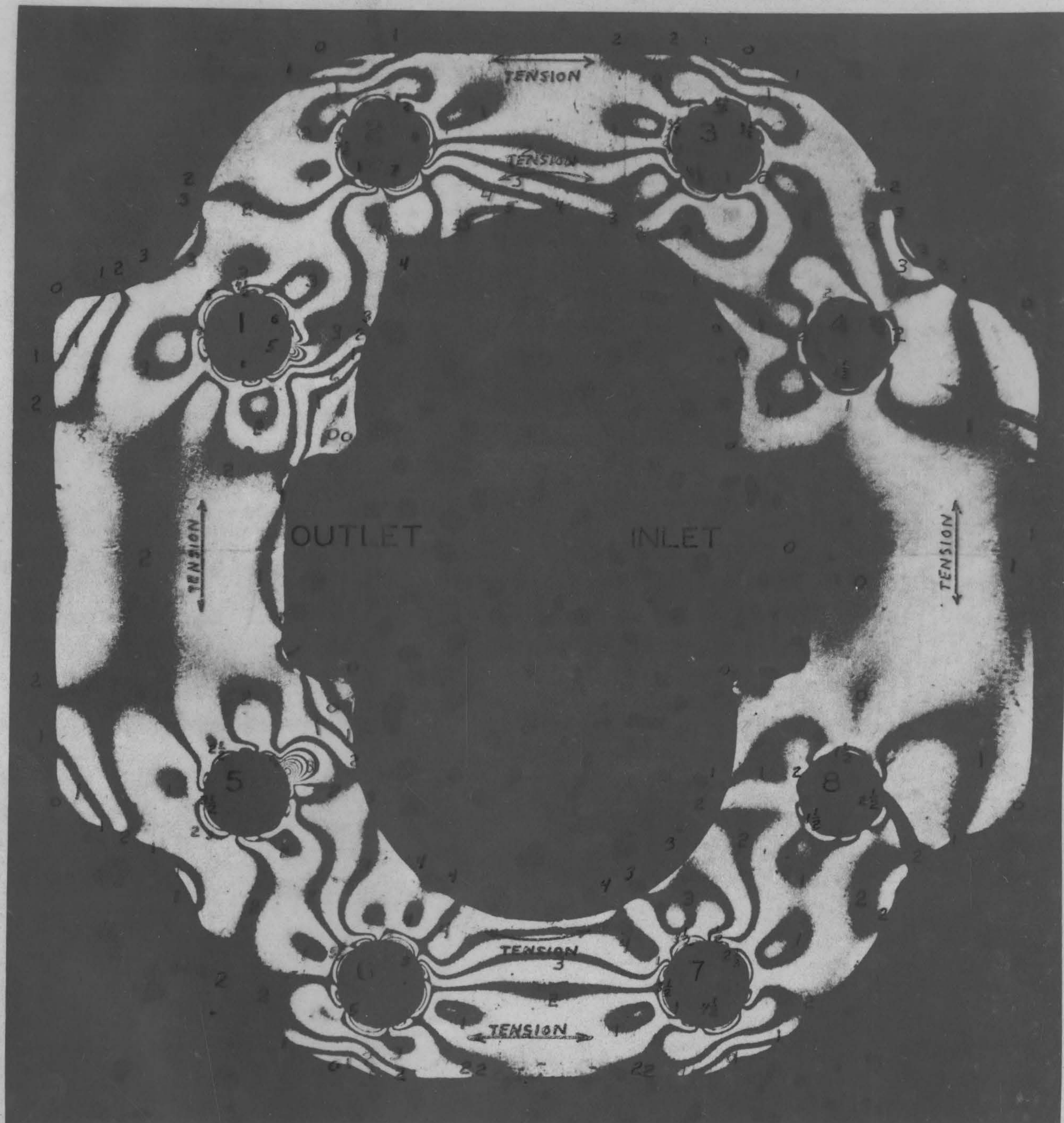

Fig. 14.--Isochromatic fringe pattern in the housing model

OVERLAY NO. 2

IDENTIFICATION OF THE FRINGES

OVERLAY NO. 3

FRINGE VALUES AT THE SURFACES

The fringe order at the surfaces of the model are recorded on overlay number 3.

The highest order fringe in the top half of the model occurs at the inside surface of hole number 2. This is a seventh order fringe and corresponds to a model stress difference ($\sigma_1 - \sigma_2$) of 59.6 psi. Since this stress occurs at a free surface exposed to atmospheric pressure $\sigma_2 = 0$ and $\sigma_1 = 59.6$ psi in the x, y plane in a direction tangent to the surface. This corresponds to a stress of 12,397 psi in the actual part. Considering that the gear housing is a continuous medium, it has been determined that the entire section has the general stress mode of tension.

The housing is made of grey cast iron (class G3000) having a tensile strength of 30,000 psi. For a static load there is a factor of safety of

$$\text{Factor of Safety} = \frac{30{,}000 \text{ psi}}{12{,}397 \text{ psi}}$$

$$\text{Factor of Safety} = 2.4$$

Considering the possibility of the pump being subjected to a cyclic load with the outlet pressure fluctuating between 100 psig and 2500 psig, the endurance limit of the

Iron is calculated[4]

$$\sigma_{endurance} = (\text{endurance limit})(\sigma_{tensile})$$

$$\sigma_{endurance} = (.4)*(30{,}000)$$

$$\sigma_{endurance} = 12{,}000 \text{ psi}$$

The factor of safety then becomes .97.

---

[4]Mechanics of Metals, Frank A. D'Isa, Addison-Wesley Publishing Company, 1968, Table 7-1, Page 322.

CHAPTER VI

CONCLUSIONS

The results of this investigation are encouraging and explain the mode of failure that is experienced in the field. That is, when an unported gear housing fractures, it does so across the bolt hole numbered 2 or 6.

For the sake of completeness, the problems encountered when testing are mentioned. The first attempt at stress freezing the model was terminated when it was discovered that the bolt force was sufficient to cause creep at the stress freezing temperature. This eliminated the internal clearance (.005 inches), made it very difficult to start the pump, and generated more heat than could be effectively removed.

For the second run, the thrust plates were machined to provide the .005 inch internal clearance, and the pump and the model were loaded prior to the heating cycle. This provided an internal pressure which acted on the end covers and counteracted a portion of the bolt force. The oven provided temperature control within 5° F as did the heat exchanger (until the oven temperature dropped below 130° F). At 130° F the loading was removed and the oven and oil allowed to cool to room temperature (5° per hour).

Based on the data obtained by this test, it is possible to make several observations:

1. The stress level decreases as the distance from the gear bore increases.
2. The entire housing experiences tension in the x-y plane.
3. The bolt holes act as stress risers; this presents a problem with cyclic loads. It should be noted that in operation the pump loading is cyclic but the number of cycles is generally small in comparison to the time the pump is in operation.
4. The lowest stress levels occur on the outside surface of the housing and in the flanges.

The following recommendations are made to increase the reliability of the design:

1. Increase the distance between the bolt holes and the gear bore.
2. The surface finish can be improved (reaming) which would inhibit the initiation of a crack.
3. The housing material could be changed from grey cast iron to a higher strength or more ductile material. For example, the endurance limit can be increased 20% by using an aluminum with the same tensile strength.

This test has been successful in establishing a better understanding of the stress patterns in an actual housing. It also provides an accurate method for determining stress levels of hydraulic components having irregular shapes and subjected to a complex form of loading.